



## WAKE-PATTERNS AND AERODYNAMIC LOADS OF A PAIR OF SIDE-BY-SIDE CIRCULAR CYLINDERS

**Bruna Oliveira Passos e Silva Siqueira**

Institute of Mechanical Engineering, Federal University of Itajubá, Av. BPS, CEP. 1303, Itajubá, MG, Brazil  
bruna.passos@gmail.com

**Alex Mendonça Bimbato**

Institute of Mechanical Engineering, Federal University of Itajubá, Av. BPS, CEP. 1303, Itajubá, MG, Brazil  
alexbimbato@yahoo.com.br

**Luiz Antonio Alcântara Pereira**

Institute of Mechanical Engineering, Federal University of Itajubá, Av. BPS, CEP. 1303, Itajubá, MG, Brazil  
luizantp@unifei.edu.br

**Abstract.** *This paper presents numerical results of two-dimensional, incompressible unsteady-flows around a pair of immovable circular cylinders in side-by-side arrangements. The vorticity field has been treated by a Lagrangian vortex method in a Reynolds number value of  $5.5 \times 10^4$ . There are two goals in this research: the first one varies the distance  $T/d$  between 0.1 and 1.3 diameters ( $d$ ) to analyze near-wake patterns and to classify them as: "single-bluff-body behavior" ( $0 < T/d < 0.1-0.2$ ), "biased flow pattern" ( $0.1-0.2 < T/d < 1-1.2$ ) and "parallel vortex street" ( $T/d > 1.2$ ). And the second one investigates temporal series history of aerodynamic loads as well as vortex-shedding frequencies for both cylinders. Vortex-shedding frequencies are calculated using two numerical probes strategically located downstream of the bodies. The numerical results obtained are in good agreement with experimental observations.*

**Keywords:** *vorticity evolution, syde-by-side arrangement, near-wake, vortex shedding frequency, Lagrangian vortex method*

### 1. INTRODUCTION

The study of the flow through two immovable cylinders in side-by-side arrangement presents characteristics of regimes of flow interference that need to be understood for better problem formulation in fluid mechanics. The unsteady vortex-structure interactions induce fluctuations in the fluid force that may be synchronized with the bodies oscillation. The surface roughness effects and their influence on Reynolds number values need to be investigated by researchers because they will shift the critical Reynolds number to lower values. Therefore, the motivation for the present study stems largely from the engineering design problem of predicting amplitudes of motion in vortex-induced cylindrical structures vibration such as nuclear power plants, heat exchangers, offshore platforms and so on. The present paper, therefore, contributes by using a Lagrangian Vortex Method in order to produce physical explanations concerning to the wake-patterns and aerodynamic loads of a pair of immovable side-by-side cylinders in high Reynolds number flows.

Zdravkovich (1987) conducted detailed studies of proximity effects and interference effects between wakes of two circular cylinders, presenting concerning discussions for in-tandem, side-by-side and staggered circular cylinders arrangements. "Figure 1" shows the flow regimes that are identified when the flow passes through a pair of circular cylinders. The first pair of cylinders on the left is arranged in side-by-side, the second group represents the in-line configuration and the last set represents the staggered configuration.

For two side-by-side circular cylinders the wake interference effects and proximity effects between bodies promote the formation of three flow regimes classified by Zdravkovich (1987) as: "single vortex street" to  $0 \leq T/d < 1.2$ , "bistable regime or biased gap flow" to  $1.2 \leq T/d < 2.2$  and "parallel vortex streets" to  $2.3 \leq T/d < 4$ . For values of  $T/d$  above 4 the "parallel vortex streets" loses intensity and disappears.

The "single vortex street" regime is characterized by a wake of vortices formed downstream of the two cylinders with the same behavior as a wake on the isolated circular cylinder. In the "bistable regime" there is the formation of two wakes classified as narrow wake (NW) and wide wake (WW). These wakes have different characteristics in respect to the aerodynamic loads and vortex shedding frequency behavior (Alam *et al.*, 2003). The third regime, so called "parallel vortex streets", also presents interesting features. Due to the distance  $T/d$ , each cylinder presents wake pattern formed independently of each other, showing similar values of aerodynamic loads and vortex shedding frequency. The results were obtained for Reynolds number varying between  $1.5 \times 10^4$  and  $9.5 \times 10^4$ . And an important observation made by Zdravkovich (1987) is that the regimes obtained for subcritical Reynolds are different from those for laminar Reynolds as presented by Williamson (1985).

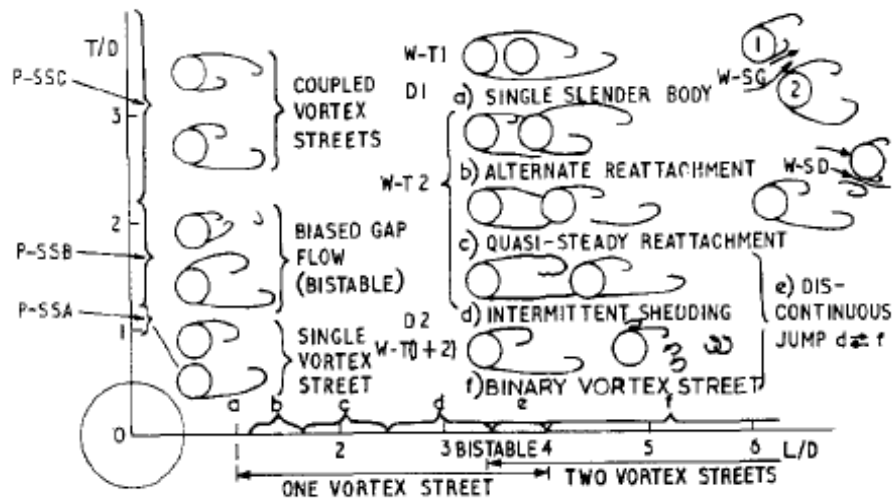


Figure 1. Flow patterns in two side-by-side circular cylinders. Reproduced from Zdravkovich (1987).

Wang & Zhou (2005) conducted experimental study by using water channel to observe hydrodynamic behavior of the flow around two side-by-side circular cylinders. It was identified the three flow regimes explained by Alam *et al.* (2003), but they discuss in detail the bistable regime in respect to the behavior of "narrow wake" and "wide wake" and the interaction between the vortices in the wake. This interaction between vortices directly influences the phenomenon of deflection of the gap flow (gap flow is the flow that develops in the space between the cylinders). The gap flow is an interaction between the shear layers which are formed on the bottom of the upper cylinder and on the top of lower cylinder, as shown in "Fig. 2". The deflection is the displacement of the gap flow in accordance with the motion trend of the flow in this space, which is probably influenced by the pressure field in this region. This work is also very rich in results, but was carried out at low Reynolds numbers varying between 230 to 750. However, the results can be used for qualitative comparison with the present numerical results for Reynolds number of  $5.5 \times 10^4$ .

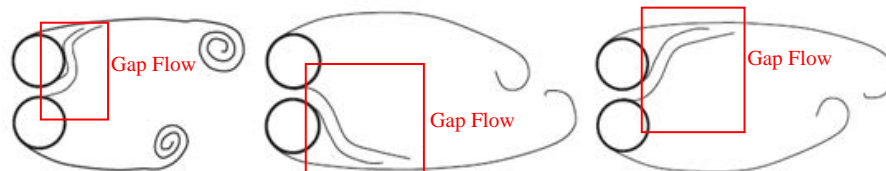


Figure 2. Gap flow between the cylinders.

Recently, Sumner (2010) presented an extensive review of experimental and numerical studies developed over the last 20 years that relate steady flow of immovable pairs of circular cylinders. It was presented the configuration for each flow patterns, the influence of Reynolds number on these patterns, the behavior of aerodynamic loads and the Strouhal number for given values of  $T/d$ .

As a basis for the development of the present work has been used the results from Alam *et al.* (2003) where they shown experimental results for a pair of side-by-side circular cylinders with Reynolds number of  $5.5 \times 10^4$  and  $T/d$  varying from 0 to 1.2, values as used herein. Alam *et al.* (2003) found for  $0 < T/d < 0.1 - 0.2$  the "single vortex street" regime, for  $0.1 - 0.2 < T/d < 1.2$  the "biased gap flow (bistable regime)" regime and for  $T/d > 1.2$  the "parallel vortex streets" regime. They present for each value of  $T/d$  chosen the behavior of aerodynamic loads, wake frequencies, pressure distribution and the images of the flow patterns. They obtain the results of aerodynamic loads and wake frequencies through the hot wire probe, but this technique implies fluctuations in the load values, in the wake frequencies and requiring more care in the post-processing of these results, as the influence of probes on the development of flow.

Important notes about NW and WW were made by Alam *et al.* (2003). The NW was classified as high frequency mode and also was concluded that this mode has higher values of drag coefficient, which is due to the proximity between the shear layers and high velocity developed on the wake. The WW was classified as low frequency mode and has a drag coefficient less than NW. As for the lift coefficients of the cylinders are explained according to the circulation around the cylinders. The counterclockwise circulation originated a positive lift force. When occurred a clockwise circulation, then there was a negative lift force.

Alam *et al.* (2003) also deny Zdravkovich (1987) when they state that the Reynolds number does not influence the flow patterns, then it may be a qualitative comparison between flows with different Reynolds numbers.

In the present paper has been collected the same results, but numerical probes were used (See “Fig. 3”), which do not influence the flow generating results without fluctuations, facilitating post-processing of results and understanding of the physical phenomena involved in the problem (Moraes *et al.*, 2012).

The numerical simulation performed in this work for Reynolds number  $5.5 \times 10^4$  and  $T/d$  varying from 0 to 1.3 showed results consistent with the experimental work of Alam *et al.* (2003).

## 2. PROBLEM FORMULATION AND NUMERICAL SOLUTION

“Figure 3” presents two side-by-side circular cylinders of diameter  $d = 2R_0$  and spaced one of other of  $T/d$ . The fluid domain ( $S$ ), which is defined by surfaces  $S_1$  (upper cylinder surface),  $S_2$  (lower cylinder surface) and  $S_3$  (surface which delimits the flow at large distances of the cylinders), is represented by  $S = S_1 \cup S_2 \cup S_3$ . The coordinate system “xoy” is fixed to the upper cylinder while the system “ $\xi O \eta$ ” is fixed to the lower cylinder and it may be movable in relation to “xoy”, allowing to impose to the lower cylinder oscillating movements in case of forced harmonic vibrations in a future work.

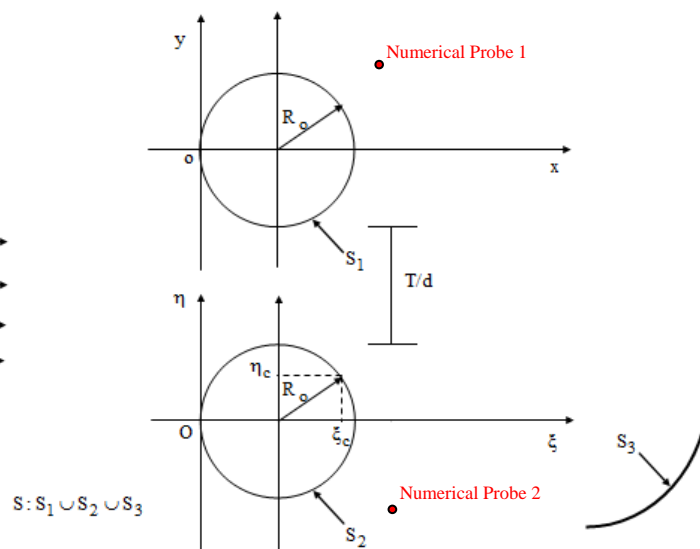


Figure 3. Geometry and definitions of the problem.

### 2.1 Governing Equations of the Problem

The problem is governed by the continuity equation and Navier-Stokes equations as shown in “Eqs. (1)” and “(2)”, respectively as

$$\nabla \cdot \mathbf{u} = 0 \quad (1)$$

$$\frac{\partial \mathbf{u}}{\partial t} + (\mathbf{u} \cdot \nabla) \mathbf{u} = -\nabla p + \nu \nabla^2 \mathbf{u} \quad (2)$$

The flow is to be considered incompressible and the fluid is Newtonian with constant properties, where  $\mathbf{u}$  is the velocity field,  $p$  is the pressure and  $\nu$  the kinematic viscosity of fluid.

### 2.2 Numeric Solution: The Lagrangian Vortex Method

The dynamics of the fluid motion is studied in a more convenient way taking the curl of the Navier-Stokes equations to obtain the vorticity equation

Silva Siqueira, B. O. P., Alcântara Pereira, L. A.  
Wake Patterns and Aerodynamic Loads of a Pair of Side-By-Side Circular Cylinders

$$\frac{\partial \omega}{\partial t} + \mathbf{u} \cdot \nabla \omega = \frac{1}{Re} \nabla^2 \omega. \quad (3)$$

where  $\omega(\mathbf{x}, t) = \nabla \times \mathbf{u}(\mathbf{x}, t)$  represents the only non-zero component of the vorticity field for 2-D flow. Note that the pressure is absent from the formulation. An algorithm that splits the convective-diffusive operator of “Eq. (3)” is employed in accordance with Chorin (1973). The Reynolds number is defined as  $Re = \frac{Ud}{\nu}$ , where  $d$  is the diameter

cylinder; the dimensionless time is  $d/U$ . The Vortex Method proceeds by discretizing spatially the vorticity field using a cloud of elemental vortices, which are characterized by a distribution of vorticity,  $\zeta_{\sigma_i}$  (commonly called the cutoff function), the circulation strength  $\Gamma_i$  and the core size  $\sigma_i$ . Thus, the discretized vorticity is expressed by

$$\omega(\mathbf{x}, t) \approx \omega^h(\mathbf{x}, t) = \sum_{i=1}^Z \Gamma_i(t) \zeta_{\sigma_i}(\mathbf{x} - \mathbf{x}_i(t)), \quad (4)$$

where  $Z$  is the number of point vortices of the cloud used to simulate the vorticity field. The numerical analysis is conducted over a series of small discrete time steps  $\Delta t$  for each of which a discrete vortex element  $\Gamma_{(i)}$  is shed from body surface. The intensity  $\Gamma_{(i)}$  of these newly generated vortices is determined using the no-slip condition on  $S_b$ . NP flat source panels represent cylinder surface to ensure impermeability condition on  $S_b$  (Katz and Plotkin, 1991).

It is assumed that the source strength per length is constant. The velocity field  $\mathbf{u}$  is calculated at the location of elemental vortices in a typical Lagrangian description. The vortex-vortex interaction is obtained from the vorticity field by means of the Biot-Savart law. The convective motion of each vortex generated on the body surface is determined by integration of each vortex path equation using a first order Euler scheme. The diffusion of vorticity is taken care of using the random walk method (Lewis, 1999).

Starting from the Navier-Stokes equations is obtained a Poisson equation for the pressure. This equation is solved through the following integral formulation (Shintani and Akamatsu, 1994).

$$H\bar{Y}_i - \int_S \bar{Y} \nabla \Xi_i \cdot \mathbf{e}_n dS = \iint_{\Omega} \nabla \Xi_i \cdot (\mathbf{u} \times \boldsymbol{\omega}) d\Omega - \frac{1}{Re} \int_S (\nabla \Xi_i \times \boldsymbol{\omega}) \cdot \mathbf{e}_n dS, \quad \bar{Y} = p + \frac{u^2}{2}, \quad u = |\mathbf{u}|, \quad (5)$$

where  $H = 1$  in the fluid domain,  $H = 0.5$  on the boundaries,  $\Xi$  is a fundamental solution of the Laplace equation and  $\mathbf{e}_n$  is the unit vector normal to the body surface,  $S_b$ . The drag and lift coefficients are obtained from pressure integration (Bimbatto *et al.*, 2011).

### 3. RESULTS

The vortex code was validated simulating the flow around an isolated circular cylinder, i.e.,  $T/d=5,000$ . This was done in order to determine the parameters associated with the numerical method, like: number of flat panels used to represent the circular cylinder (NP=300); position of detachment of the discrete vortices ( $\epsilon_{ps} = 0.0010$ ); Lamb core size ( $\sigma_o = 0.0010$ ). The simulation was performed with 1000 advances in time with time increment  $\Delta t = 0.05$  showing consistent results, coming to the classical Von Kármán street of two cylinders in the end thereof, as shown in "Fig. 4".

With this information at hand it is concluded that the code is able to simulate two side-by-side circular cylinders with proximity and interference effects to check the flow patterns mentioned above.

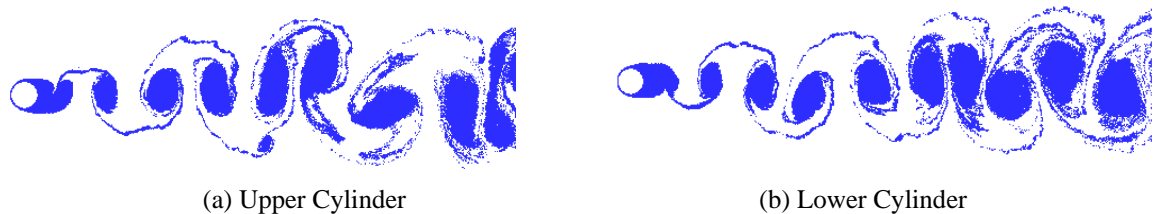


Figure 4. Von Kármán vortex street formed in two circular cylinders for  $T/d=5,000$ .

An special attention was given to the biased gap flow regime because it is a rich regime in physical phenomena. In the present work the biased gap flow was found for  $T/d = 0.1$  and  $T/d = 0.5$ , as presented by Alam *et al.* (2003).

As discussed earlier in the biased gap flow regime there are two types of wakes the narrow wake (NW) and wide wake (WW) and second Alam *et al.* (2003) these flow patterns are changed randomly each other, i.e., there isn't an exact tendency for their occurrence only in the lower or upper cylinder. This behavior is called "switching phenomena".

The drag ( $\overline{C_D}$ ) and lift ( $\overline{C_L}$ ) coefficients and the Strouhal number of the upper and lower cylinders for the biased gap flow are shown in "Tab. 1". The subscripts U and L accompanying parameters correspond to the upper and lower cylinders respectively.

Table 1. Aerodynamic coefficients and Strouhal number of two side-by-side cylinders at  $Re=5.5 \times 10^4$ .

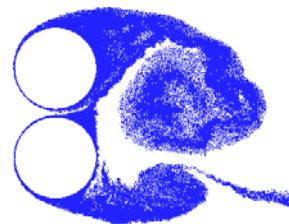
T/d	$\overline{C_{DU}}$	$\overline{C_{LU}}$	$\overline{C_{DL}}$	$\overline{C_{LL}}$	$St_{wKU}$	$St_{wKL}$	Flow pattern classification
5,000	1.22	-0.08	1.22	-0.08	0.21	0.19	Von Kármán street
0.1	1.54	0.26	1.54	-0.18	0.20	0.20	Transition to biased gap flow
0.5	1.28	0.25	1.18	-0.15	0.12	0.13	Biased gap flow
1.3	1.36	0.21	1.26	-0.08	0.21	0.21	Parallel vortex street

For  $T/d = 0.1$  is observed transition from the single vortex street for the biased gap flow which is characterized by higher values of drag coefficients of the two cylinders in relation to the isolated cylinder which has  $\overline{C_D} = 1.22$ . Alam *et al.* (2003) calculating their results as a function of the results NW ( $\overline{C_D} = 1.69$  e  $\overline{C_L} = -0.12$ ) and WW ( $\overline{C_D} = 1.21$  e  $\overline{C_L} = 0.61$ ).

In the present paper there is a transition between regimes and it was observed that the results tend to values of NW in the lower cylinder with respect to the range of  $\pm 10\%$  error, while in the upper cylinder there is a tendency to the formation of WW due to highest  $\overline{C_{LU}}$  value. In the "Fig. 5" there is a comparison between the results of Alam *et al.* (2003) and the present simulation. Note that these wakes have the same behavior, including the deflection of the gap flow that is deflected upward, confirming a good response from the numerical code.



(a) Alam *et al.* (2003)



(b) Present Simulation

Figure 5. Comparison between experimental and numerical results for wake pattern.

The Strouhal number ( $St$ ) behaved as expected, for  $T/d = 0.1$ , Alam *et al.* (2003) found for two side-by-side cylinders the same value of the isolated cylinder  $St = 0.186$ . In this simulation the Strouhal numbers for the two cylinders are equal to the isolated cylinder  $St = 0.20$  simulated by this code.

The second case was simulated  $T/d = 0.5$  which showed very interesting results. Due to the distance between the cylinders NW and WW manifest themselves clearly. The influence of the deflection of the gap flow in behavior of the cylinders wakes is also observed leading to switching phenomena.

The behavior of aerodynamic loads is depicted in "Fig. 6" for both cylinders. A first analysis leads to the conclusion that the two cylinders have the same behavior. But analyzing the "Tab. 1", the drag and lift coefficients of the upper cylinder ( $\overline{C_{DU}}$  e  $\overline{C_{LU}}$ ) are different from the coefficients of the lower cylinder ( $\overline{C_{DL}}$  e  $\overline{C_{LL}}$ ). This difference is due to the switching phenomena.

The switching phenomena results from the alternation between the NW and WW wakes which causes another phenomenon, the coalescence between the vortex structures formed in wakes of the two cylinders. This phenomenon was observed by Wang & Zhou (2005) and during post processing of the results of this simulation this phenomenon

Silva Siqueira, B. O. P., Alcântara Pereira, L. A.  
Wake Patterns and Aerodynamic Loads of a Pair of Side-By-Side Circular Cylinders

also manifested. The coalescence presents a random behavior, sometimes occurs in the wake of the upper cylinder and sometimes occurs in the wake of the lower cylinder. These results from the influence of the gap flow which depends on the pressure field generated in the region between the cylinders.

The "Figure 7" shows the development process of the phenomenon of coalescence from the wake of the upper cylinder. At time  $t = 25.60$  of simulation there is the formation of a clockwise vortex structure on the top of the upper cylinder. At time  $t = 27.25$  are formed a counterclockwise vortex structure on the bottom of the upper cylinder and a clockwise vortex structure on top of the lower cylinder, the latter two structures interact generating the gap flow. The first structure formed in the upper cylinder increases its intensity making the gap flow is deflected upward (See "Fig. 7.c") carrying the generated structure on top of the lower cylinder (See "Figure 7.d"). At this point in the simulation the three structures coalesce leading to a unique vortex structure (See "Fig. 7.e") that has circulation cut by a new vortex structure that begins to rise on the bottom of the lower cylinder.

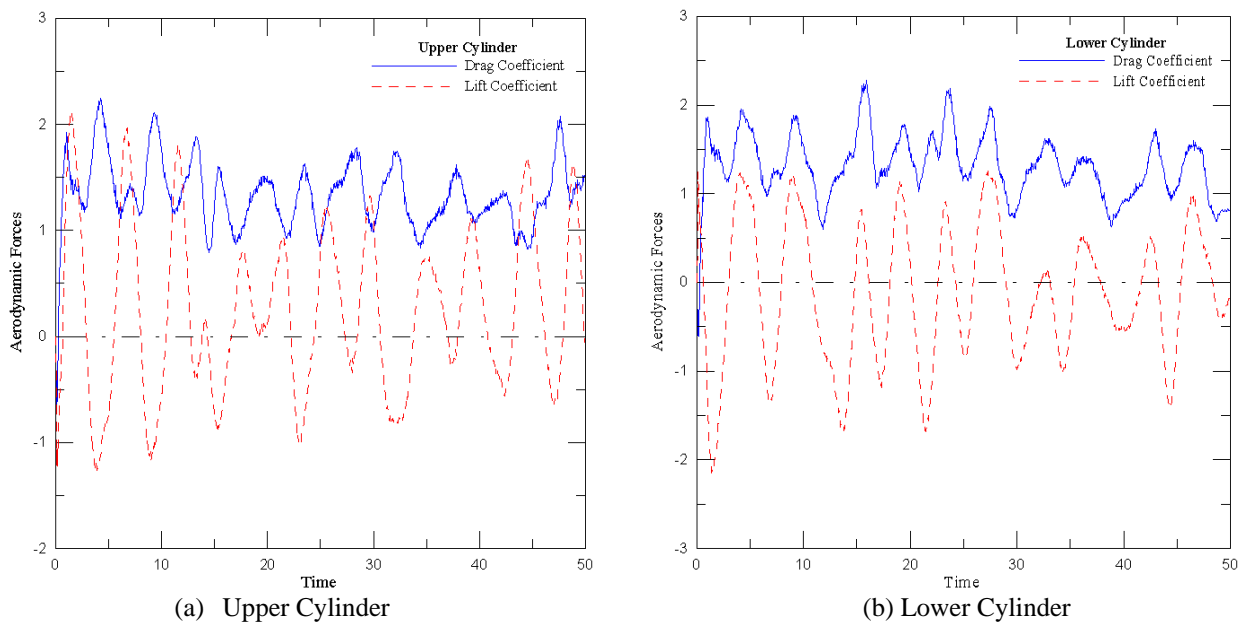


Figure 6. Aerodynamic loads of a pair of side-by-side circular cylinders for  $T/d = 0.5$ .

Coalescence in the wake of the lower cylinder (see "Fig.8") occurs in the same manner as described above, but the deflection of the gap flow is inclined downwards, according to "Fig. 8.c". The switching phenomena can be observed at this point in the discussion. It is evident in "Fig. 7.c" a narrow wake in the upper cylinder (NW) and a wider wake in the lower cylinder (WW). Already in "Fig. 8.c" the WW is located in the upper cylinder and the NW in the lower cylinder. This behavior changes modes on the wakes and characterizes the switching phenomena. One final note with respect to this phenomenon is that it occurs continuously on the wake and comparing "Figs. 7 and 8" note that the coalescence process, although occur at different times, behaves in mirrored form.

All phenomena involved in the formation of the biased gap flow are a direct consequence of the pressure field that develops around the surface of the cylinders and the wake vortices. Therefore, it was studied the pressure distribution at instants determined in "Figs. 7 and 8" shown in "Figs. 9 and 10".

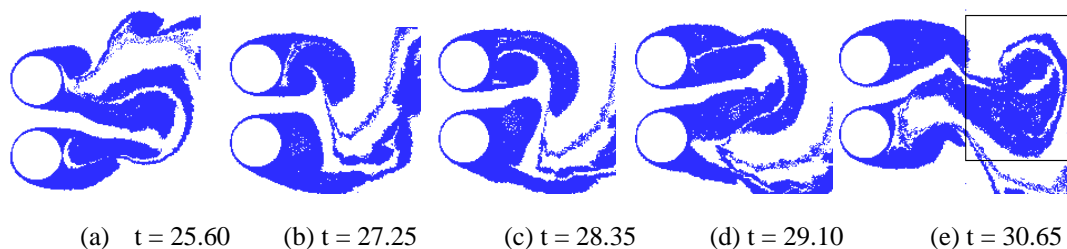


Figure 7. Phenomenon of coalescence in the wake of the upper cylinder for  $T/d = 0.5$ .

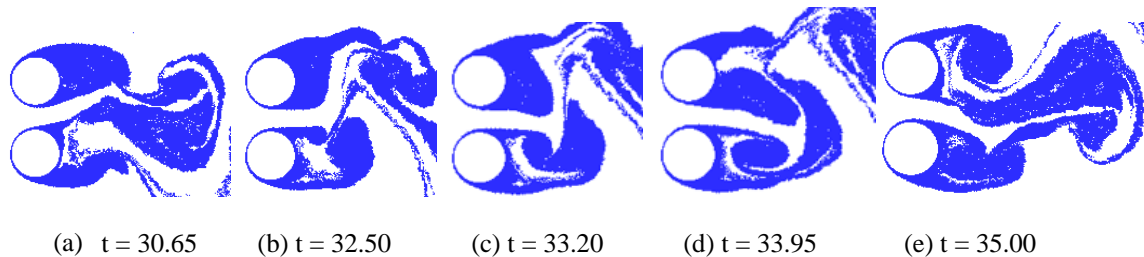


Figure 8. Phenomenon of coalescence in the wake of the lower cylinder for  $T/d = 0.5$ .

"Figure 9" presents the distribution of instantaneous pressure for the coalescence in the wake of the upper cylinder. At time  $t=25.60$  (see "Fig. 9.a") is observed a region of low pressure that occurs around  $60^\circ$  causing a peak of lift leading to the birth of a vortex structure on the outside of the upper cylinder. At time  $t=27.25$  there is the birth of a vortex structure at the bottom of the upper cylinder around  $260^\circ$  triggered by a minimal peak in the lift curve and simultaneously arises a vortex structure on top of the lower cylinder around  $60^\circ$ . At time  $t=28.35$  the gap flow starts to develop and there is a pressure approximately equal to the region between the cylinders. Upon reaching the instant  $t=29.10$  pressure distribution at the top of the lower cylinder (region around  $60^\circ$ ) is greater than the pressure distribution on the bottom of the upper cylinder (region around  $260^\circ$ ) which causes the gap flow to deflect up carrying the vortex structure in the lower cylinder that comes off completely to wake the instant  $t=30.65$ . For the case of coalescence in the wake of the lower cylinder, the process is the same, but the distribution of pressures occur in opposite directions causing the gap flow deflect downward.

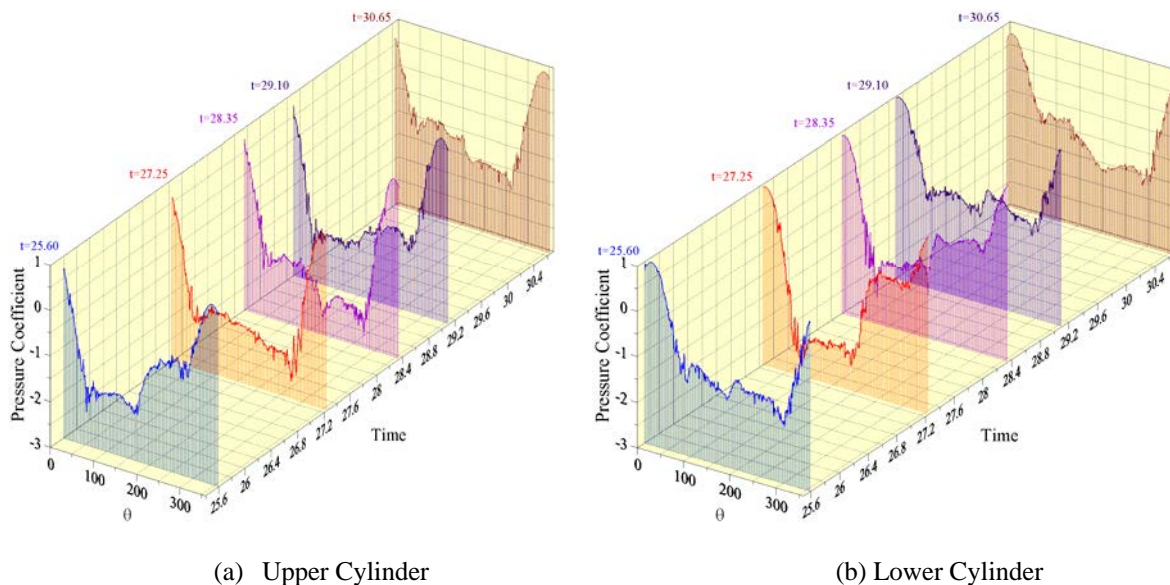


Figure 9. Instantaneous pressure distribution for identification of coalescence in the wake of the upper cylinder for  $T/d = 0.5$ .

In the "Fig. 10" is presented the distribution of instantaneous pressure for the coalescence in the wake of the lower cylinder. At time  $t=30.65$  is a region of low pressure around  $60^\circ$ , causing a peak maximum of the lift curve leading to birth of a vortex structure in the outside of the lower cylinder. At time  $t=32.50$  a vortex structure born on top of the lower cylinder  $60^\circ$  a result of a minimum peak in the lift curve and simultaneously arises a vortex in the bottom of the upper cylinder around  $260^\circ$ . At the instant  $t=33.20$  the gap flow develops and there is a pressure approximately equal to the region between the cylinders.

At time  $t=33.95$  the pressure distribution on the bottom of the upper cylinder (region around  $260^\circ$ ) is greater than the pressure distribution at the top of the lower cylinder (region around  $60^\circ$ ), then the gap flow deflects downward carrying the vortex structure of the upper cylinder that comes off completely to the wake in time  $t=35.00$ .

Silva Siqueira, B. O. P., Alcântara Pereira, L. A.  
Wake Patterns and Aerodynamic Loads of a Pair of Side-By-Side Circular Cylinders

For  $T/d = 0.5$ , dominant Strouhal number found by Alam *et al.* (2003) was 0.11. In the present simulation the value of Strouhal dominant has been identified as 0.12 to the upper cylinder and 0.13 to the lower one (See "Tab. 1"), which shows the capacity of the code to reproduce satisfactory results.

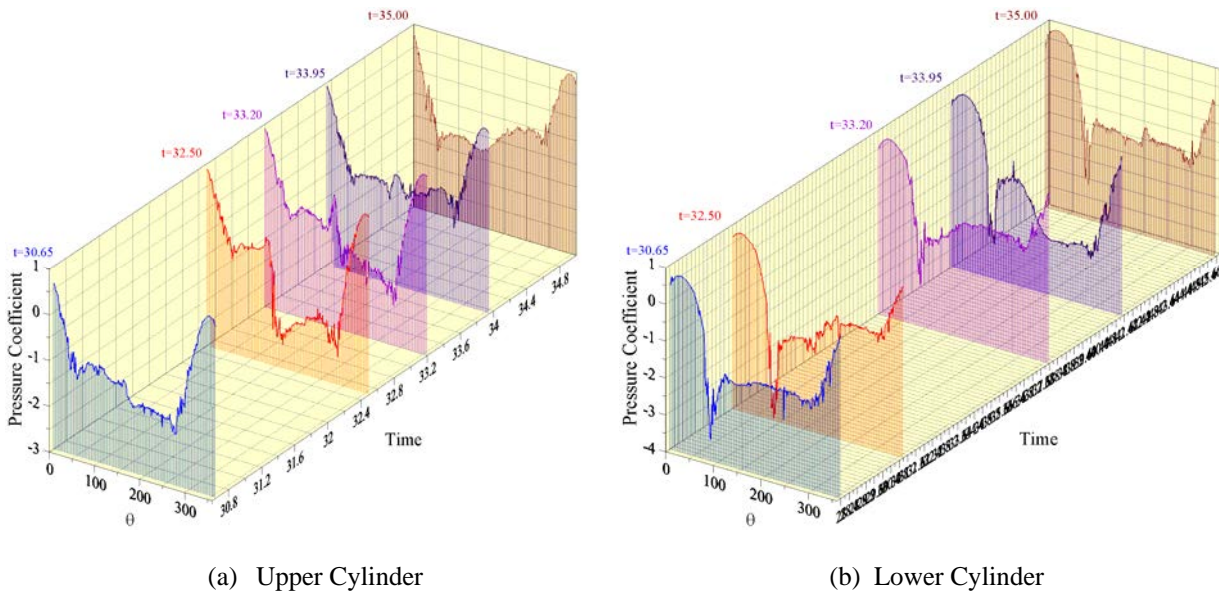


Figure 10. Instantaneous pressure distribution for identification of coalescence in the wake of the lower cylinder for  $T/d = 0.5$ .

The latter case corresponds to simulated  $T/d = 1.3$ . Alam *et al.* (2003) noted in his work that for values of  $T/d > 1.2$  the wakes of cylinders present Strouhal numbers very close to the Strouhal of isolated cylinder and it occurs in this simulation. In the "Tab. 1" can be observed that the values obtained for each cylinder are in accordance with proposed by the authors.

For  $T/d = 1.3$  was verified the "parallel vortex streets" regime. Zdravkovich (1987) noted in this regime that each cylinder has a wake formed independently of each other and parallel having the same frequency of vortex shedding in wake ( $St_{W_{KU}} = St_{W_{KL}}$ ), which is also observed in the present simulation. The drag coefficients, although not the same, are very close, considering a range of  $\pm 10\%$  of uncertain.

The behavior of the aerodynamic loads is shown in "Fig. 11" and the vortex wakes formed in each cylinder are in "Fig. 12" which shows that the vortices detach themselves out of phase, i.e., there is a delay in the vortex shedding of upper cylinder than the lower.

The vortex shedding out of phase between the cylinders can be explained by pressure distribution in the cylinder surface. The distribution of instantaneous pressure of the points A to E present in "Fig. 11" is shown in "Fig. 13" and note that it is around the lower cylinder that pressure field shows lower values than the pressure field around the upper cylinder. This difference is one of the reasons for this discrepancy between wakes.

A phenomenon that can also be used to explain this delay is the Venturi effect, as there is a contraction of the flow area in the region between the cylinders, there is a pressure drop and an increase in this speed, which advances the detachment structures in vortex structures in the lower cylinder, this phenomenon may be the key answer to this difference between the pressure fields.

The same behavior is observed for  $T/d = 5,000$ . Although the case has been simulated for checking the behavior of isolated body was observed at this stage out of phase shedding of wakes, where the wake in the lower cylinder is advanced over the top.

In this case it is not possible to use the Venturi effect as justification for the interaction between the pressure field, then it is assumed that this is an intrinsic characteristic of two side-by-side circular cylinder.

In the "Fig. 14" is a comparison between the results obtained by Alam *et al.* (2003) and the present simulation for  $T/d = 1.3$  and in both cases the shedding is noted the out of phase shedding of wakes, again confirming the results obtained in the present numerical simulation.

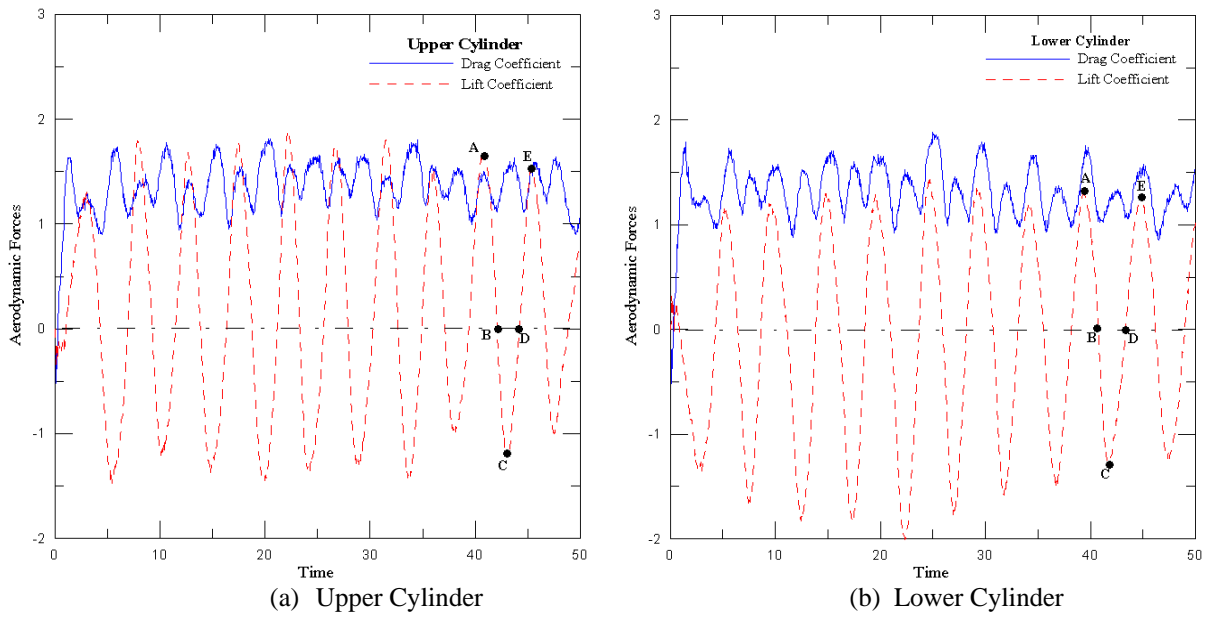


Figure 11. Aerodynamic loads of a pair of side-by-side circular cylinders for  $T/d = 1.3$ .



Figure 12. Vortex wake at time  $t = 45.35$ .

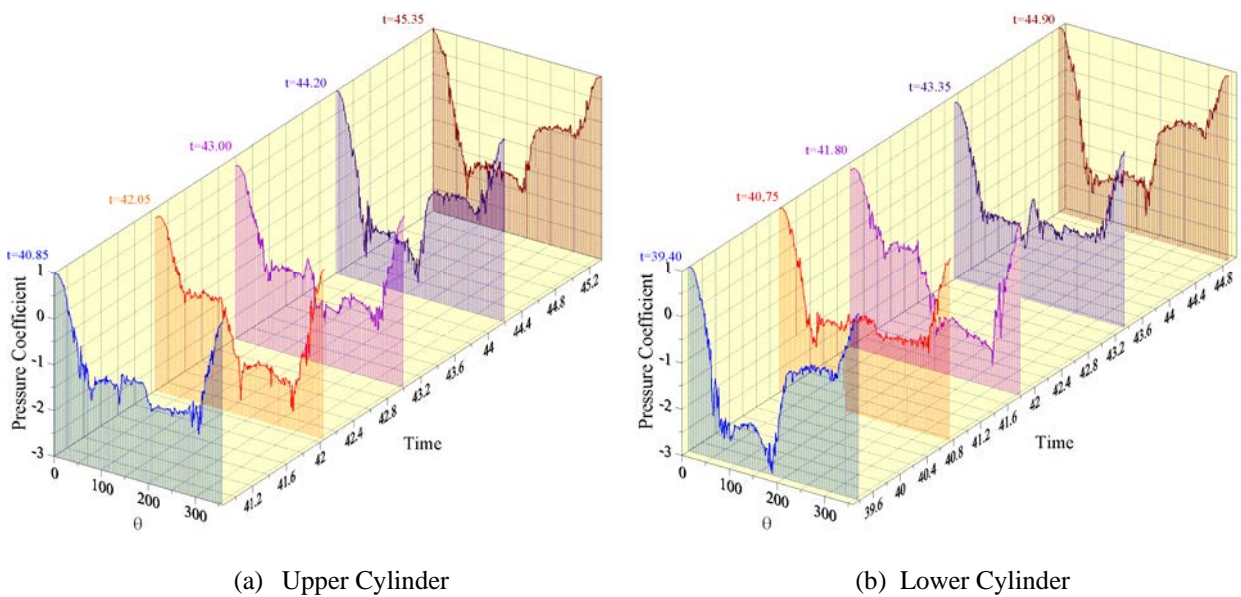


Figure 13 – Instantaneous pressure distribution for the surface of the cylinders for  $T/d = 1.3$ .

Silva Siqueira, B. O. P., Alcântara Pereira, L. A.  
Wake Patterns and Aerodynamic Loads of a Pair of Side-By-Side Circular Cylinders

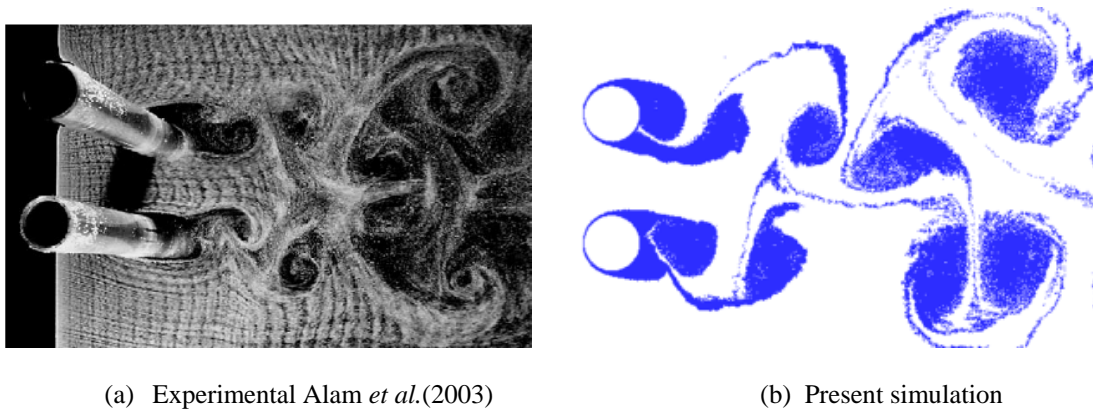


Figure 14. Comparison between the experimental results of Alam *et al.* (2003) and the results of this simulation for  $T/d = 1.3$ .

#### 4. CONCLUSIONS

In the present work the Lagrangian Vortex Method was used for flow simulation at high Reynolds number through two immovable side-by-side circular cylinders. The aim was to analyze the flow patterns in the wake of the cylinders.

The regimes discussed in depth were bistable regime flow and parallel vortex street that have more complex physical phenomena and must be increasingly studied due to the complexity of these flows. The present results were satisfactory and showed good agreement with the one presented by Alam *et al.* (2003) in a physical sense.

Finally in the near future a roughness modeling will be incorporated to the numerical method to investigate the regimes of vortex formation when a rough cylinder oscillates and its surface is heated.

#### 5. REFERENCES

- Bimbato, A. M., Alcântara Pereira, L. A., Hirata, M. H., 2011. "Study of the Vortex Shedding Flow around a Body near a Moving Ground", *Journal of Wind Engineering & Industrial Aerodynamics*, Vol. 99, pp. 7-17.
- Chorin, A.J., 1973, "Numerical Study of Slightly Viscous Flow", *Journal of Fluid Mechanics*, Vol. 57, pp. 785-796.
- Katz, J. and Plotkin, A., 1991. "Low Speed Aerodynamics: From Wing Theory to Panel Methods". McGraw Hill, Inc.
- Lewis, R.I., 1999, "Vortex Element Methods, the Most Natural Approach to Flow Simulation - A Review of Methodology with Applications", *Proceedings of 1st Int. Conference on Vortex Methods*, Kobe, Nov. 4-5, pp. 1-15.
- Mahbub Alam, Md., Moriya, M. and Sakamoto, H., 2003. "Aerodynamic Characteristics of Two Side-by-Side Circular Cylinders and Application of Wavelet Analysis on the Switching Phenomenon". *Journal of Fluids and Structures*, Vol. 18, pp. 325-346.
- Moraes, P.G., Alcântara Pereira, L. A., Hirata, M. H., 2012. "The Formation of Binary-Vortex Street Behind Two Circular Cylinders Arranged in Tandem", *14<sup>th</sup> Brazilian Congress of Thermal Engineering and Sciences, Proceedings of ENCIT 2012*, Rio de Janeiro, Brazil, November 18-22.
- Shintani, M. and Akamatsu, T., 1994, "Investigation of Two Dimensional Discrete Vortex Method with Viscous Diffusion Model", *Computational Fluid Dynamics Journal*, Vol. 3, No. 2, pp. 237-254.
- Sumner, D., 2010. "Two circular cylinders in a cross-flow: A review". *Journal of Fluids and Structures*, Vol. 26, pp. 849-899.
- Wang, Z.J., Zhou, Y., 2005. "Vortex Interactions in a Two Side-by-Side Cylinder Near-Wake". *International Journal of Heat and Fluid Flow*, Vol. 26, pp. 362-377
- Williamson, C.H.K., 1985. "Evolution of a Single Wake Behind a Pair of Bluff Bodies". *Journal of Fluid Mechanics*, 159, pp. 1-18.
- Zdravkovich, M. M., 1987. "The Effects of Interference Between Circular Cylinders in Cross Flow". *Journal of Fluids and Structures*, Vol. 1, pp. 239-261.

#### 6. RESPONSIBILITY NOTICE

The authors are the only responsible for the printed material included in this paper.